PHYSICAL REVIEW B **75**, 241203(R) (2007)

Origins of the doping asymmetry in oxides: Hole doping in NiO versus electron doping in ZnO

Stephan Lany, Jorge Osorio-Guillén, and Alex Zunger
National Renewable Energy Laboratory, Golden, Colorado 80401, USA
(Received 23 February 2007; published 14 June 2007)

The doping response of the prototypical transparent oxides NiO (*p*-type), ZnO (*n*-type), and MgO (insulating) is caused by spontaneous formation of compensating centers, leading to Fermi-level pinning at critical Fermi energies. We study the doping principles in these oxides by first-principles calculations of carrier-producing or -compensating defects and of the natural band offsets, and identify the dopability trends with the ionization potentials and electron affinities of the oxides. We find that the room-temperature free-hole density of cation-deficient NiO is limited by a too large ionization energy of the Ni vacancy, but it can be strongly increased by extrinsic dopants with shallower acceptor levels.

DOI: 10.1103/PhysRevB.75.241203 PACS number(s): 61.72.Vv, 61.50.Nw, 71.15.Nc

It was once thought that wide-gap materials such as oxides cannot be doped (see review in Ref. 1). We now know that they can be doped, but also that there exists a fundamental asymmetry with respect to the dopability by electrons (*n*-type behavior) and by holes (*p*-type behavior). For example, ZnO (E_g=3.4 eV at room temperature) is readily dopable by electrons, but hardly by holes, whereas NiO [E_g=3.7 eV (Ref. 2)] is readily dopable by holes [3] but not by electrons. This doping asymmetry is accompanied by an asymmetry in nonstoichiometry towards anion deficiency in ZnO,[4,5] but towards cation deficiency in NiO.[3,4] The enormous electron concentrations (of the order of 10^{21} cm^{-3}) achievable by donor doping in ZnO render it a prototype "*n-type* transparent conductive oxide" (TCO),[6] whereas NiO is a prototype *p-type* TCO,[7,8] especially when alloyed with Co.[9] In classic inorganic chemistry,[4] such trends in off-stoichiometry are explained qualitatively by considering the stable oxidation states of the cation: For example, the existence of a stable, higher oxidation state of Ni [Ni(III), as in (Ni_2O_3)] relative to Ni(II) in NiO suggests that it is possible to have on average fewer than one Ni atom per oxygen, leading to a Ni deficiency of NiO. However, such arguments do not explain the microscopic origin of nonstoichiometry (e.g., the formation of Ni vacancies V_{Ni} or oxygen-interstitials O_i) or its implication for electrical properties, such as the creation of free carriers. It is now understood[10] what are the material conditions needed for a wide-gap oxide to be an electron-hole conductor: (i) Electron- (hole-) producing defects—i.e., either intrinsic defects, such as vacancies or interstitials, or extrinsic impurities—should be abundant in *n*-type (*p*-type) systems—i.e., have low formation energies. (ii) Such donors (acceptors) must be readily ionized—i.e., have energetically shallow electrical levels. (iii) "Electron killers" such as the cation vacancy or "hole killers" such as the anion vacancy, which oppose doping by electrons and holes, respectively, should not develop spontaneously—i.e., should have high formation energies.

In the present work, we investigate by means of defect theory the origins of the fundamental doping asymmetry in the prototype *p*- and *n*-type TCO's, NiO and ZnO, respectively, in the light of oxide nonstoichiometry: We calculate the formation energies of electron (hole) producers and of electron (hole) killers for NiO, ZnO, and for MgO, as a reference for a prototypical insulating oxide. In subsequent thermodynamic simulations, we determine for NiO the cation deficiency and free-hole densities in the pure and in the Li-doped oxide. By calculating the natural band offsets between the studied oxides, we establish the general trend that a large electron affinity—i.e., a low energy of the conduction band minimum (CBM)—facilitates *n*-type doping, because the formation energy of electron killers (e.g., metal vacancies) stays high even when the Fermi energy E_F is close to the CBM. Similarly, a small ionization potential—i.e., a high energy of the valence band maximum (VBM)—facilitates *p*-type doping, because the formation energy of hole killers (e.g., O vacancies V_O) stays high, even when E_F is close to the VBM.

Critical Fermi-level pinning energies limit doping. Imagine that we deliberately introduce electrons into the host crystal via some sort of intrinsic or extrinsic doping, or by electron injection. This raises the Fermi energy E_F towards the CBM. Since the formation energy $\Delta H(E_F)=\Delta H(0)+qE_F$ of intrinsic, charged defects ($q\neq 0$) is a function of E_F,[10] it becomes easier to form negatively charged ($q<0$) acceptors (e.g., V^{2-}_{cation}) the higher E_F rises in the gap.[10] Eventually, at a sufficiently high Fermi level $E_F^{\boldsymbol{n},\mathrm{pin}}$, the formation energy of host acceptors (A="electron killers") will vanish, $\Delta H_A(E_F^{\boldsymbol{n},\mathrm{pin}})=0$, and these electron killers will form spontaneously and halt the deliberate *n*-type doping. Similarly, the introduction of holes into the lattice lowers E_F towards the VBM, so that at a critical Fermi level $E_F^{\boldsymbol{p},\mathrm{pin}}$, the host donor ($D$="hole killers") formation energy vanishes, $\Delta H_D(E_F^{\boldsymbol{p},\mathrm{pin}})=0$, and such hole killers (e.g., V_O or the cation interstitial cat_i) form spontaneously and halt the deliberate *p*-type doping. Thus, the response of the host to external doping is uniquely characterized by the critical Fermi energies $E_F^{\boldsymbol{n},\mathrm{pin}}$ and $E_F^{\boldsymbol{p},\mathrm{pin}}$, which are determined in the following.

Calculation of defects. Using a supercell representation, we calculate the defect formation energy of a defect D in charge state q as

$$\Delta H_{D,q}(E_F,\mu)=[E_D-E_H]+q\cdot E_F+\Sigma n_\alpha(\mu_\alpha^0+\Delta\mu_\alpha), \quad (1)$$

where E_D and E_H are the total energies of the host+defect and host-only supercells, respectively. We calculate the total energy via the pseudopotential momentum-space formalism,

as implemented in the VASP code,[11] and apply our general scheme to correct for errors associated with the local density or generalized gradient approximation (LDA or GGA) and with the use of finite supercells, as described in detail in the Appendix of Ref. 12. The present results are based on the GGA, as parametrized in Ref. 13. Defects are calculated using 64-atom supercells of (antiferromagnetic) NiO and (nonmagnetic) MgO in the rocksalt structure. In wurzite ZnO, defects were calculated[5] in 72-atom supercells. The chemical potentials $\Delta\mu_{\mathrm{Ni}}$, $\Delta\mu_{\mathrm{Mg}}$, $\Delta\mu_{\mathrm{Zn}}$, and $\Delta\mu_{\mathrm{O}}$ for atoms α added to $(n_\alpha=-1)$ or removed from $(n_\alpha=+1)$ the lattice to form defect D are taken with respect to the energy μ_α^0 of the elementary metals and the O_2 molecule. From the calculated $\Delta H_{D,q}$, we determine, as a function of temperature and oxygen partial pressure $P(O_2)$, the equilibrium defect and carrier concentrations via thermodynamic simulations.[5,14]

Correction of the erroneous NiO phase instability in GGA. In addition to the notorious underestimation of band gap energies in the LDA and GGA [the band gap of NiO is only 0.66 eV in the GGA, compared to the measured value of 3.7 eV (Ref. 2)], we find for NiO another important shortcoming of the GGA pertinent to our study: In contrast to experiment,[15] the GGA predicts NiO to be unstable with respect to the formation of Ni_2O_3 (assuming the corundum structure). In thermodynamic equilibrium, the Ni and oxygen chemical potentials must satisfy the stability condition for NiO, $\Delta\mu_{\mathrm{Ni}}+\Delta\mu_{\mathrm{O}}=\Delta H_{\mathrm{f}}(\mathrm{NiO})$, where ΔH_{f} is the calculated NiO formation enthalpy. However, the inequality $2\Delta\mu_{\mathrm{Ni}}+3\Delta\mu_{\mathrm{O}}\leqslant\Delta H_{\mathrm{f}}(\mathrm{Ni_2O_3})$ is violated in the GGA for all $(\Delta\mu_{\mathrm{Ni}}\leqslant 0,\ \Delta\mu_{\mathrm{O}}\leqslant 0)$ pairs that satisfy the NiO stability condition, implying that, over the whole range of growth conditions, NiO is unstable with respect to Ni_2O_3. In principle, a global LDA-GGA correction approach, such as *GW* or self-interaction correction, is expected to fix simultaneously all LDA-GGA errors. Here, we use instead the GGA+U scheme,[16] in which the correction is artificially restricted to a given atom and a given angular momentum. We select for the Ni d shell the Coulomb and exchange energy parameters as $U=4.3$ eV and as $J=1.0$ eV, respectively, such that the experimental phase stability of NiO with respect to Ni_2O_3 is recovered (i.e., Ni_2O_3 forms only at strongly O-rich conditions $\Delta\mu_{\mathrm{O}}\geqslant -0.10$ eV). The respective value of the band gap in GGA+U is $E_g=2.32$ eV. A larger value $U=8$ eV for the Coulomb parameter, as deduced from constrained LDA calculations,[17] leads to a band gap closer to experiment, but has been found to be too large for optical properties (dielectric function),[18] and the thermodynamic stability (Ref. 19 and the present work). Note also that the GGA+U approach for the Ni d shell cannot be expected to correct the full band gap error in NiO, as evidenced by fact that band gaps are underestimated in the LDA and GGA even for systems without transition-metal d states (e.g., Si, GaAs). In ZnO, we found[5] that the VBM shifts downward by 0.69 eV due to GGA+U with $U-J=7$ eV. We used this parameter also here for the band offset calculations.

Abundance of intrinsic defects. Figure 1 shows the calculated formation energies for the intrinsic defects in NiO, ZnO, and MgO. We find that lattice vacancies are generally the most important defects in the considered oxides: Under O-rich (metal-poor) conditions (Fig. 1, left), Ni vacancies have a low $\Delta H<1$ eV, even when E_{F} is close to the VBM, indicating that V_{Ni}, not the O interstitial, is the main channel of nonstoichiometry in NiO. In contrast, the metal vacancies in ZnO and MgO have a higher $\Delta H\approx 3$ eV when E_{F} is close to the VBM, and only when E_{F} is well inside the gap does their formation energy become low. This indicates that metal vacancies are not the main channel of nonstoichiometry in ZnO, but they exist mainly as charged, compensating acceptors (electron killers)—e.g., in n-type ZnO.[5] Under O-poor (metal-rich) conditions (Fig. 1, right), O vacancies have low formation energies ~ 1 eV, implying significant V_{O} concentrations, but they do not produce free electrons due to their deep donor levels (note, however, that we predicted in Ref. 20 a *metastable* shallow state of V_{O} in ZnO causing persistent photoconductivity).

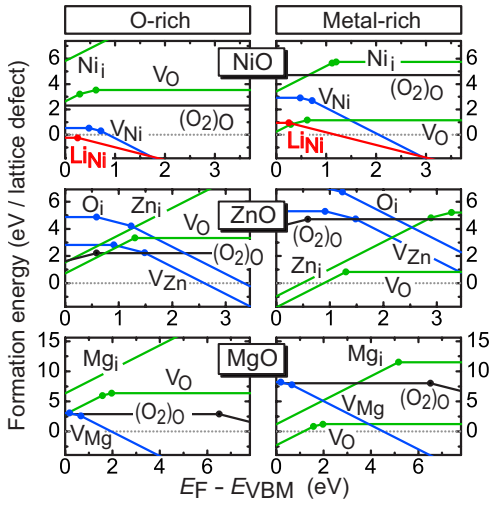

FIG. 1. (Color online) Defect formation energies in NiO, ZnO (Ref. 4), and MgO. The dots mark transition levels between different charge states (see Ref. 26). Oxygen-rich (metal-poor) conditions are defined by the formation of the limiting phases Ni_2O_3, ZnO_2, and MgO_2, respectively. Note that under realistic growth conditions $[T>400\ \mathrm{K},\ P(O_2)\leqslant 1\ \mathrm{atm}]$, the O chemical potential is limited by the O_2 gas phase. Metal-rich conditions are defined by the limiting metallic Ni, Zn, and Mg phases. The Li chemical potential is limited by the formation of Li_2O.

Even though the potential hole killer V_{O} in NiO can be abundant under O-poor conditions, its formation energy stays high under the O-rich condition generally conducive to p-doping (Fig. 1). Thus, p-doping of NiO is not hindered by compensation due to intrinsic donors; i.e., condition (iii) above is satisfied for p-doping of NiO. This is illustrated in Fig. 2(a), where the results of our thermodynamic simulations for the defect concentrations $c(V_{\mathrm{Ni}})$ and $c(V_{\mathrm{O}})$ and for the hole densities $p(T)$ are compared with experiment:[3,21] The calculated results agree within one order of magnitude with the experimental data and show the same temperature dependence, indicating that the observed free holes are indeed caused by thermal formation and ionization of Ni vacancies. The concentration of V_{O} hole killers stays low except for high temperatures $(T_g>1500\ \mathrm{K})$, where the decrease[14] of the O chemical potential $\Delta\mu_{\mathrm{O}}$ with temperature at constant $P(O_2)$ leads to lower V_{O} formation energies.

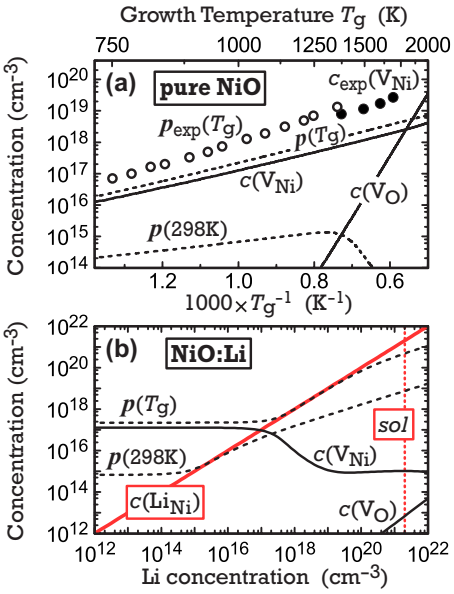

FIG. 2. (Color online) (a) Calculated and experimental (Refs. 3 and 21) concentrations of defects and free-holes (p) for equilibrium growth of pure NiO, as a function of the growth temperature T_g. The calculated hole densities are given both for T_g and for 298 K after thermal quenching. (b) Calculated defect and free-hole densities for Li-doped NiO grown at T_g=1000 K, as a function of the Li-dopant concentration. The vertical dashed line ("sol") indicates the calculated Li solubility limit. Both in (a) and (b), we consider O-rich conditions [$P(O_2)$=1 atm] which support hole doping.

Fermi level pinning energies on a common energy scale. Since the doping response of NiO, ZnO, and MgO is reflected in the Fermi-level pinning energies $E_F^{n,\mathrm{pin}}$ and $E_F^{p,\mathrm{pin}}$, we calculate the band offsets, shown in Fig. 3, to place these pinning energies on a common energy scale. The "strained" valence band offset between two materials A and B is determined as[22]

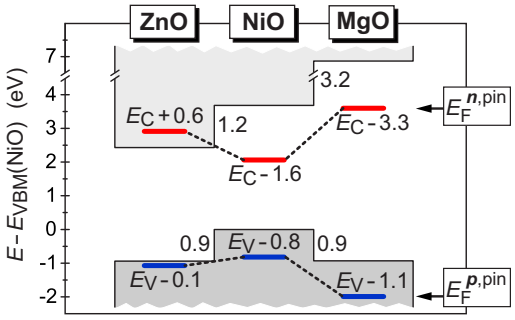

FIG. 3. (Color online) Calculated "natural" band offsets between ZnO, NiO, and MgO (cf. Table I), along with the respective Fermi-level pinning energies $E_F^{n,\mathrm{pin}}$ and $E_F^{p,\mathrm{pin}}$, which describe the upper and lower limits, respectively, of the equilibrium Fermi level, as imposed by the formation of compensating defects. $E_F^{n,\mathrm{pin}}$ is determined for metal-rich conditions ($\Delta\mu_{\mathrm{metal}}$=0), which facilitate n-doping, while $E_F^{p,\mathrm{pin}}$ is determined for O-rich conditions facilitating p-doping [$P(O_2)$=1 atm, T_{growth}=1000 K].

TABLE I. Calculated strained (average in-plane lattice constant) and natural band offsets ΔE^{vbm} in eV between rocksalt NiO and MgO, and zinc-blende ZnO. Note that the NiO/MgO interface is naturally unstrained due to their similar lattice constants.

	Strained	Natural
NiO/ZnO	−0.58	−0.94
NiO/MgO	−0.93	−0.93
MgO/ZnO	0.18	0.24

$$\Delta E^{\mathrm{vbm}}(A/B) = [\bar{V}_B(A/B) - \bar{V}_A(A/B)] + (\varepsilon_B^{\mathrm{vbm}} - \varepsilon_A^{\mathrm{vbm}}), \quad (2)$$

where $\bar{V}_A(A/B)$ and $\bar{V}_B(A/B)$ are the average electrostatic potentials within the A and B parts of the A/B superlattice (the average of the calculated A and B lattice constants is used for the in-plane directions). The VBM energies $\varepsilon_A^{\mathrm{vbm}}$ and $\varepsilon_B^{\mathrm{vbm}}$ with respect to the average potential are determined in the biaxially strained individual binary materials A and B. Equation (2) also describes the ionization potential (IP) of, e.g., material B, when replacing material A by vacuum and setting $\varepsilon_A^{\mathrm{vbm}}$=0. Thus, using the vacuum level as an absolute reference, we determine the "natural" (i.e., unstrained) band offset by calculating the change of the IP when the biaxial strain is released. Table I gives the strained and natural band offsets between NiO, ZnO, and MgO. Here, we considered the zinc-blende structure for ZnO in which the atoms are tetrahedrally coordinated, similar as in wurzite ZnO.[23]

Large electron affinities facilitate n-type oxides. Figure 3 compares the trends in dopability—i.e., condition (iii) above—using the natural valence band offsets and the experimental band gap energy for the conduction band offsets. We find that only in ZnO is $E_F^{n,\mathrm{pin}}=E_C+0.6$ eV *inside the conduction band*. Thus, the propensity for high n-dopability of ZnO relies on the fact that the V_{Zn} electron killer forms spontaneously only when E_F is already well inside the conduction band, so the system is already highly n-type, before compensation occurs. This resilience of ZnO against formation of the electron killer V_{Zn} is supported by the relatively large electron affinity (low CBM energy; see Fig. 3). In contrast, NiO and MgO are not n-dopable, since the pinning levels $E_F^{n,\mathrm{pin}}=E_C-1.6$ eV and $E_C-3.3$ eV, respectively, lie well below the CBM. Thus, the spontaneous annihilation of electron doping due to the formation of the electron killers V_{Ni} and V_{Mg} is due to their smaller electron affinity.

Small ionization potentials facilitate p-type oxides. The p-type pinning levels $E_F^{p,\mathrm{pin}}=E_V-0.1$ −0.8, and −1.1 eV, for ZnO, NiO, and MgO, respectively, lie all inside the valence band, indicating that p-type doping is possible as far as the spontaneous formation of hole killers is concerned. However, the achievement of actual p-type conductivity requires additionally the abundance of acceptors with shallow ionization energies—i.e., conditions (i) and (ii) above. In case of high VBM energies (small IPs), such as found here for NiO, the primary defect states of the cation vacancy (the O−p-like dangling bonds), occur as resonances inside the valence band rather than as deep gap states.[24] Such resonances lead to the formation of secondary defect levels in the gap, which are

host derived and delocalized acceptors states conducive to *p*-type conductivity.[20] In contrast, the lower VBM energy (larger IP) in ZnO and MgO places the primary cation-vacancy levels inside the gap, leading to deep and localized acceptor levels[25] [cf. Fig. 1 (see Ref. 26)]. Thus, condition (ii) above of reasonably small ionization energies is generally difficult to achieve in materials with large IP, such as ZnO and MgO. Finally, condition (i) above of low acceptor formation energies is also supported by a small IP, since ΔH of negatively charged defects (acceptors) decreases when the energy E_V of the VBM is raised [cf. Eq. (1)].

Increasing the free-hole densities by extrinsic doping. Figure 2(a) shows the actual room-temperature free-hole density $p(298\ \mathrm{K})$ in pure NiO, after high-temperature equilibrium growth. We see that $p(298\ \mathrm{K}) \leqslant 10^{15}\ \mathrm{cm}^{-3}$ stays well below the concentration of V_{Ni} acceptors [Fig. 2(a)] and the respective high-temperature hole density $p(T_g)$. The reason is that the transition levels of V_{Ni}, $\varepsilon(0/-)=E_V+0.48$ eV and $\varepsilon(-/2-)=E_V+0.72$ eV, are not shallow enough to ionize most V_{Ni} acceptors at room temperature. Therefore, we considered hole doping through the *extrinsic* hole producer (Refs. 3 and 8): The low formation energy $\Delta H(\mathrm{Li_{Ni}}) \leqslant 1$ eV (Fig. 1, red line) leads to a high equilibrium solubility—e.g., $c(\mathrm{Li})=2\times10^{21}\ \mathrm{cm}^{-3}$ at $T=1000$ K and $P(\mathrm{O_2})=1$ atm. For these growth conditions, Fig. 2(b) shows the calculated defect and hole densities, as a function of the Li concentration. We see that, in particular, the room-temperature hole density is significantly higher than for pure NiO [cf. Fig. 2(a)], approaching $10^{19}\ \mathrm{cm}^{-3}$ toward the Li solubility limit [Fig. 2(b)]. This higher free-hole density results mainly from the shallower $\varepsilon(0/-)=E_V+0.25$ eV level of the $\mathrm{Li_{Ni}}$ acceptor.

Summary. (a) NiO is *p* dopable, because the hole killer V_{O} is sufficiently unstable under appropriate conditions. Yet, the free-hole density at ambient temperature is low in pure NiO, because the acceptor levels of the hole producer V_{Ni} are not close enough to the VBM to ionize most vacancies. Doping by extrinsic impurities such as Li, however, can largely increase the free-hole density. (b) NiO is not *n*-dopable, because the electron killer V_{Ni} forms spontaneously before significant levels of electrons are introduced by doping.

Note added in proof. Recently, Janotti and van de Walle[27]calculated the isostructural wurzite-wurzite MgO/ZnO natural band-offset of $\Delta E^{\mathrm{vbm}}=1.2$ eV, considerably larger than our heterostructural rocksalt-zincblende value of 0.24 eV (Table I). In order to directly compare iso- and heterostructural offsets, we calculated also the natural band-offset for the isostructural zincblende-zincblende MgO/ZnO interface, finding indeed a larger value $\Delta E^{\mathrm{vbm}}=0.93$ eV than for the heterostructural band offset. This comparison indicates that there is a considerable VBM offset $\Delta E^{\mathrm{vbm}}=-0.7$ eV between the natural octahedral (rocksalt) and the hypothetical tetrahedral (zincblende, wurzite) structure of MgO.

This work was funded by the U.S. Department of Energy, DOE-EERE, under Contract No. DE-AC36-99GO10337.

[1] J. A. van Vechten, in *Handbook of Semiconductors*, edited by S. P. Keller (North-Holland, Amsterdam, 1980).

[2] R. J. Powell and W. E. Spicer, Phys. Rev. B **2**, 2182 (1970); Z. Zhang, Y. Zhao, and M. Zhu, Appl. Phys. Lett. **88**, 033101 (2006).

[3] F. J. Morin, Phys. Rev. **93**, 1199 (1953).

[4] P. Kofstadt, *Non-Stoichiometry, Diffusion, and Electrical Conductivity in Binary Metal Oxides* (Wiley, New York, 1972); D. M. Smyth, *The Defect Chemistry of Metal Oxides* (Oxford University Press, Oxford, 2000).

[5] S. Lany and A. Zunger, Phys. Rev. Lett. **98**, 045501 (2007).

[6] *Transparent Conducting Oxides*, edited by D. S. Ginley and C. Bright [MRS Bull. **25** (2000)].

[7] H. Sato *et al.*, Thin Solid Films **236**, 27 (1993).

[8] U. S. Joshi *et al.*, Appl. Surf. Sci. **252**, 2524 (2006).

[9] C. F. Windisch, Jr. *et al.*, Thin Solid Films **420–421**, 89 (2002).

[10] A. Zunger, Appl. Phys. Lett. **83**, 57 (2003).

[11] J. Ihm, A. Zunger, and M. L. Cohen, J. Phys. C **12**, 4409 (1979); G. Kresse and D. Joubert, Phys. Rev. B **59**, 1758 (1999).

[12] C. Persson, Y. J. Zhao, S. Lany and A. Zunger, Phys. Rev. B **72**, 035211 (2005).

[13] J. P. Perdew, K. Burke, and M. Ernzerhof, Phys. Rev. Lett. **77**, 3865 (1996).

[14] J. Osorio-Guillen, S. Lany, S. V. Barabash, and A. Zunger, Phys. Rev. Lett. **96**, 107203 (2006).

[15] *CRC Handbook of Chemistry and Physics*, 87th ed. (Taylor & Francis, Boca Raton, 2007).

[16] V. I. Anisimov, I. V. Solovyev, M. A. Korotin, M. T. Czyzyk and G. A. Sawatzky, Phys. Rev. B **48**, 16929 (1993).

[17] V. I. Anisimov, J. Zaanen, and O. K. Andersen, Phys. Rev. B **44**, 943 (1991).

[18] O. Bengone, M. Alouani, P. Blochl, and J. Hugel, Phys. Rev. B **62**, 16392 (2000).

[19] L. Wang, T. Maxisch, and G. Ceder, Phys. Rev. B **73**, 195107 (2006).

[20] S. Lany and A. Zunger, Phys. Rev. B **72**, 035215 (2005).

[21] S. Mrowec and Z. Grzesik, J. Phys. Chem. Solids **65**, 1651 (2004).

[22] R. G. Dandrea, C. B. Duke, and A. Zunger, J. Vac. Sci. Technol. B **10**, 1744 (1992).

[23] The rocksalt-rocksalt interface of NiO/MgO is calculated using a (001) superlattice, whereas the rocksalt–zinc-blende interfaces of NiO/ZnO and MgO/ZnO are calculated for a (112) superlattice, thereby avoiding the large electric fields present at the respective (001) interface.

[24] H. Raebiger, S. Lany, and A. Zunger, Phys. Rev. B (to be published).

[25] D. Galland and A. Herve, Phys. Lett. **33A**, 1 (1970); Y. Chen and M. M. Abraham, J. Phys. Chem. Solids **51**, 747 (1990).

[26] The rather shallow transition levels of V_{Mg} in MgO, shown in Fig. 1, are an artifact of the GGA and reflect the general difficulty of density functional methods to describe Jahn-Teller systems and holes localized on single O atoms in oxides [cf. J. Lægsgaard and K. Stokbro, Phys. Rev. Lett. **86**, 2834 (2001)]. The deeper levels of V_{Zn} in ZnO are obtained due to the downshift of the VBM in the GGA+U method, but do not reflect the Jahn-Teller distortion.

[27] A. Janotti and C. G. van de Walle, Phys. Rev. B **75**, 121201 (2007).